



|                  |  |
|------------------|--|
| Title            | Effects of human amnion-derived mesenchymal stromal cell transplantation in rats with radiation proctitis  |
| Author(s)        | Ono, Masayoshi; Ohnishi, Shunsuke; Honda, Minori; Ishikawa, Marin; Hosono, Hidetaka; Onishi, Reizo; Nakagawa, Koji; Takeda, Hiroshi; Sakamoto, Naoya   |
| Citation         | Cytotherapy, 17(11), 1545-1559<br><a href="https://doi.org/10.1016/j.jcyt.2015.07.003">https://doi.org/10.1016/j.jcyt.2015.07.003</a>  |
| Issue Date       | 2015-11  |
| Doc URL          | <a href="http://hdl.handle.net/2115/63375">http://hdl.handle.net/2115/63375</a>  |
| Rights           | © 2015. This manuscript version is made available under the CC-BY-NC-ND 4.0 license<br><a href="http://creativecommons.org/licenses/by-nc-nd/4.0/">http://creativecommons.org/licenses/by-nc-nd/4.0/</a> |
| Rights(URL)      | <a href="http://creativecommons.org/licenses/by-nc-nd/4.0/">http://creativecommons.org/licenses/by-nc-nd/4.0/</a>  |
| Type             | article (author version)   |
| File Information | manuscript.pdf   |



[Instructions for use](#)

# **Effect of Human Amnion-Derived Mesenchymal Stem Cell Transplantation in Rats with Radiation Proctitis**

**Running title:** Amnion mesenchymal stem cells for radiation proctitis

Masayoshi Ono,<sup>1</sup> Shunsuke Ohnishi,<sup>1</sup> Minori Honda,<sup>2</sup> Marin Ishikawa,<sup>1,3</sup>

Hidetaka Hosono,<sup>1</sup> Reizo Onishi,<sup>1</sup> Koji Nakagawa,<sup>2</sup> Hiroshi Takeda,<sup>2</sup>

and Naoya Sakamoto<sup>1</sup>

<sup>1</sup>Department of Gastroenterology and Hepatology, Hokkaido University Graduate School of Medicine, Sapporo, Japan

<sup>2</sup>Laboratory of Pathophysiology and Therapeutics, Faculty of Pharmaceutical Sciences, Hokkaido University, Sapporo, Japan

<sup>3</sup>Department of Cancer Pathology, Hokkaido University Graduate School of Medicine, Sapporo, Japan.

**Corresponding Author:**

Dr. Shunsuke Ohnishi, Department of Gastroenterology and Hepatology, Hokkaido

University Graduate School of Medicine, N15, W7, Kita-ku, Sapporo 060-8638, Japan.

E-mail: [sonishi@pop.med.hokudai.ac.jp](mailto:sonishi@pop.med.hokudai.ac.jp)

Telephone: +81-11-716-1161

Fax: +81-11-706-7867

**ABSTRACT**

**Background:** Mesenchymal stem cells (MSCs) have been reported to be a promising cell source in cell therapy, and large amounts of MSCs can easily be isolated from human amnion. Therapeutic irradiation for intrapelvic cancer often causes radiation proctitis; however, there is currently no effective treatment. We therefore investigated the effect of transplantation of human amnion-derived MSCs (AMSCs) in rats with radiation proctitis.

**Methods:** Amnion was obtained at cesarean delivery, and AMSCs were isolated and expanded. Sprague-Dawley rats were  $\gamma$ -irradiated (5 Gy/day) at the rectum for 5 days. On day 5, AMSCs ( $1 \times 10^6$  cells) were intravenously transplanted. Rats were sacrificed on day 8. Histological analyses were performed, and mRNA expression of inflammatory mediators was measured. *In vitro*, after  $\gamma$ -irradiation of rat intestinal epithelial cells (IEC-6), the cells were cultured with AMSC-conditioned medium (CM). The effect of AMSC-CM was evaluated by measuring caspase-3/7 activity, p53 transcription activity, and quantitative RT-PCR for p53-target genes.

**Results:** Histological examination demonstrated that epithelial injury and infiltration of inflammatory cells in the rectum were significantly suppressed by transplantation of AMSCs. *In vitro*, the cell injury in IEC-6 cells induced by  $\gamma$ -irradiation was inhibited by

AMSC-CM, which also inhibited the upregulation of p53 transcription activity, caspase-3/7 activity, and p21 expression.

**Conclusion:** Transplantation of AMSCs improved radiation proctitis, possibly through inhibition of cell injury and inflammatory reactions. AMSC transplantation should be considered as a new treatment for radiation proctitis.

**Keywords:** Mesenchymal stem cells, Amnion, Radiation proctitis, Cell injury.

**Abbreviations:**

AMSCs, amnion-derived mesenchymal stem cells

CM, conditioned medium

EDTA, ethylenediaminetetraacetic acid

FBS, fetal bovine serum

FM, fetal membrane

MEM, minimal essential medium

MPO, myeloperoxidase

MSCs, mesenchymal stem cells

PAS, periodic acid-Schiff

PBS, phosphate-buffered saline

RT, radiation therapy

RT-PCR, reverse transcription-polymerase chain reaction

## INTRODUCTION

Radiation therapy (RT) is frequently used for pelvic malignancies such as prostate and cervical cancer; however, RT also induces acute and chronic injury to the normal tissue.

Radiation proctitis is one of the most common side-effects in patients receiving RT for intrapelvic cancer [1, 2]. Early reactions occurring in 50%–78% of the patients include diarrhea, defecation disorders, and anal pain; late reactions occurring in about 80% of the patients include hemorrhage, with stenosis occurring in about 1%, and fistula formation occurring in 0.4% of the patients [3-6]. Treatment for early reactions includes suppository, osmotic laxative, and enema therapy; treatment for late reactions includes topical application of formalin, hyperbaric oxygen therapy, argon plasma coagulation, and operation [7, 8]. Early reactions are generally reversible; however, late reactions are irreversible, and treatments for this pathology remain unsatisfactory [9]. Therefore, development of alternative treatment is needed. Preclinical studies provide encouraging proof of concept regarding the therapeutic potential of stem cells for treating the adverse side effects associated with radiotherapy [10].

Mesenchymal stem cells (MSCs) are multipotent cells that can differentiate into a variety of lineages, including bone, cartilage, or fat, and are present in many tissues [11]. At present, MSCs have been investigated as cell sources for regenerative

medicine because of their differentiation ability and their potential to improve damaged tissues by secreting a variety of growth factors and anti-inflammatory molecules [12, 13]. The efficacy of autologous and allogeneic MSC transplantation in patients with inflammatory bowel disease has recently been reported [14, 15]. Systemic MSC therapy of three patients with refractory pelvic irradiation damages was safe and effective on pain, hemorrhage and inflammation with a long-term effect in inhibition of chronic inflammation as well as fistulization [16].

The fetal membrane (FM) consists of the amnion and chorion, which envelops the developing fetus. Although the FM is generally discarded as medical waste after delivery, fetal tissues have been found to be rich sources of MSCs [17-20]. We and others have reported that, in rats or mice, systemic administration of amnion-derived MSCs (AMSCs) improved hindlimb ischemia [21], myocarditis [22,23], glomerulonephritis [24], ischemia/reperfusion-induced acute kidney injury [25], graft-versus-host disease [26], and severe colitis [27], by inducing angiogenesis and anti-inflammatory effects.

In this study, we investigated whether the administration of human AMSCs improves radiation proctitis in rats and explored the mechanisms underlying this.



## MATERIALS AND METHODS

### *Isolation and Expansion of Human AMSCs*

The Medical Ethical Committee of Hokkaido University Graduate School of Medicine, Sapporo, Japan approved this research, and all pregnant women gave written informed consent. Human FMs were obtained during Cesarean deliveries, and the amnion was manually peeled from the chorion. AMSCs were isolated and expanded by digestion with collagenase type III (Worthington Biochemical Corporation, Lakewood, NJ, USA), followed by seeding in uncoated plastic dishes with minimal essential medium (MEM)  $\alpha$  (Life Technologies, Carlsbad, LA, USA) supplemented with 10% fetal bovine serum (FBS; Life Technologies), 100 U/mL of penicillin, and 100 ng/mL of streptomycin (Wako Pure Chemical Industries, Osaka, Japan). Cell cultures were maintained at 37°C in a humidified atmosphere of 95% air and 5% CO<sub>2</sub>. After 3–4 days in culture, non-adherent cells were removed and adherent cells were maintained in culture until they reached 80% confluence. The passage was performed using 0.5% trypsin/EDTA (Life Technologies).

### *Differentiation of AMSCs into Adipocytes and Osteocytes*

AMSCs were seeded onto six-well plates and differentiation into adipocytes and osteocytes was induced when the AMSCs were 80%–90% confluent. To induce differentiation into adipocytes, AMSCs were cultured with hMSC Mesenchymal Stem Cell Adipogenic Differentiation Medium (Lonza, Basel, Switzerland), according to the manufacturer's instructions. After 3 weeks of differentiation, cells were stained with 10  $\mu\text{g}/\text{mL}$  BODIPY 493/503 (Life Technologies) and 10  $\mu\text{M}$  Hoechst 33342 (Life Technologies). To induce differentiation into osteocytes, AMSCs were cultured in hMSC Mesenchymal Stem Cell Osteogenic Differentiation Medium (Lonza), according to the manufacturer's instructions. After 2 weeks of differentiation, cells were stained with 10  $\mu\text{g}/\text{mL}$  calcein (Dojindo Laboratories, Kumamoto, Japan). Fluorescent images were obtained using a fluorescent microscope (BZ-9000, Keyence, Osaka, Japan).

#### *Flow Cytometry*

Cultured AMSCs were harvested with 0.5% trypsin/EDTA and stained using the Human MSC Analysis Kit (Becton, Dickinson and Company (BD), Franklin Lakes, NJ, USA), which included phycoerythrin (PE)-conjugated CD44, allophycocyanin (APC)-conjugated antibody against CD73, fluorescein-isothiocyanate (FITC)-conjugated antibody against CD90, and PerCP-Cy5.5-conjugated antibody

against CD105 as well as a negative cocktail (PE-conjugated CD11b, CD19, CD34, CD45, and HLA-DR), according to manufacturer's instructions. Cells were analyzed by flow cytometry (FACSCanto II; BD).

### *Animals*

The experimental protocol was approved by the Animal Care and Use Committees of Hokkaido University. Seven-week-old male Sprague-Dawley rats were procured from Japan SLC (Hamamatsu, Japan); three rats were housed per cage in a temperature-controlled room (24°C) on a 12 h/12 h-light/dark cycle. All rats had *ad libitum* access to standard pellets.

### *Induction of Radiation Proctitis*

Rats were anesthetized by intraperitoneal injection of 50 mg/kg pentobarbital (Kyoritsu Seiyaku, Tokyo, Japan) and placed in the supine position under a 6-mm thick lead shield with a 3 × 4-cm opening around the anus (Fig. 1A). Radiation proctitis was induced by  $\gamma$ -irradiation (5 Gy/day; Hitachi Power Solutions, Ibaraki, Japan) for 5 days (day 1 through day 5, Fig. 1B). In the Control group, rats were injected with 50 mg/kg pentobarbital but not  $\gamma$ -irradiated.

### *Transplantation of Human AMSCs*

One-million human AMSCs suspended in 200  $\mu$ L of phosphate-buffered saline (PBS, Life Technologies) were intravenously transplanted through the penile vein on day 5 ( $N = 11$ ) immediately after the final irradiation (Fig. 1B); 200  $\mu$ L of PBS was injected in the Control ( $N = 6$ ) and Radiation groups ( $N = 11$ ).

### *Histological Examination*

All rats were sacrificed on day 8. The rectum was removed, fixed in 40 g/L of formaldehyde saline, embedded in paraffin, and cut into 5- $\mu$ m sections. Tissue sections were stained with hematoxylin and eosin (H&E) and periodic acid-Schiff (PAS), and microscopically examined by an independent observer. Ten consecutive fields from the anus were photographed ( $\times 40$ ) and the number of PAS-positive goblet cells was counted. Histological scoring was performed by an independent observer, according to a previous report [28]. The inflammation score was based on an estimate of polymorphonuclear leucocyte infiltration of the bowel wall; 0 = none, 1+ = infiltration confined to the mucosa, 2+ = mucosa plus minimal submucosal infiltrate, 3+ = PMN aggregates in submucosa, and 4+ = muscularis propria infiltration. Vascularity was scored by

estimating the degree of filling of blood vessels and by erythrocyte escape from the vessels: 0 = normal control, 1+ = dilation of vessels with erythrocyte stasis, 2+ = erythrocyte diapedesis, 3+ = local interstitial hemorrhage, and 4+ = extensive hemorrhage. Mucus cell loss was evaluated on PAS-stained sections. In control intestine, mucus-containing cells were found from the base of the crypts to the tips of the villi. With progressive damage, mucus cells were diminished. Scoring was as follows; 0 = mucus cells present in the full length of villi, 1+ = mucus cells present in 75% of the length, 2+ = mucus cells present in 50% of the length, 3+ = mucus cells present in 25% of the length, and 4+ = no mucus cells present.

#### *Immunohistochemical Examination*

Tissue sections were stained with anti-rat CD68 monoclonal antibody (dilution, 1:50; AbD Serotec, Kidlington, UK) and anti-myeloperoxidase (MPO) antibody (dilution, 1:300; Thermo Scientific, Waltham, MA, USA), respectively, for 40 min. Five consecutive fields from the anus were photographed ( $\times 20$ ) and the areas of CD68- and MPO-positive cells were measured, respectively (Lumina Vision, Mitani Corporation, Tokyo, Japan). Tissue sections were also stained with anti-human CD105 antibody (dilution, 1: 50; Novus Biologicals, Littleton, CO, USA), to investigate the existence of

transplanted AMSCs.

*RNA Isolation and Quantitative Reverse-Transcription Polymerase Chain Reaction (qRT-PCR)*

Total RNAs of the rat rectum and cultured rat intestinal epithelial cells (IEC-6) were extracted using the RNeasy Mini Kit (Qiagen, Hilden, Germany); 1 µg of the total RNA was reverse-transcribed into cDNA using the QuantiTect Reverse Transcription Kit (Qiagen). PCR amplification was performed using a 25-µL reaction mixture that contained 1 µL of cDNA and 12.5 µL of Platinum SYBR Green PCR Mix (Life Technologies). β-actin mRNA amplified from the same samples served as an internal control. After initial denaturation at 95°C for 2 min, a two-step cycle procedure was used (denaturation at 95°C for 15 s, annealing and extension at 60°C for 1 min) for 40 cycles in a 7700 Sequence Detector (Applied Biosystems, Foster City, CA, USA). Gene expression levels were determined using the comparative threshold cycle (ddCt) method, using β-actin as an internal control. Data were analyzed with Sequence Detection Systems software (Applied Biosystems). Primer sequences are shown in Table 1.

*Collection of Conditioned Medium (CM) from Human AMSC Culture*

AMSCs were cultured in a complete medium until the cells reached a sub-confluent state. After washing with PBS three times, cells were further cultured with serum-free MEM $\alpha$  for 48 h. Next, the CM was collected and centrifuged at  $400 \times g$  for 5 min; the supernatant was stored at  $-80^{\circ}\text{C}$  until use.

#### *Assessment of Cell Injury*

IEC-6 cells were plated in a white-walled 96-well plate at a density of  $3 \times 10^3$  cells per well and cultured with 100  $\mu\text{L}$  of complete medium. The following day, the medium was changed to AMSC-CM or serum-free medium immediately after the irradiation (4 Gy or 8 Gy). After 24 hrs, cells were incubated with Caspase-Glo 3/7 reagent (Promega, Madison, WI, USA) and the enzymatic activity of caspase-3/7 was measured using the Glo-Max Multi Detection System (Promega). Cell viability was measured by trypan blue staining (Life Technologies) and cell proliferation was measured by analyzing the cellular level of 3-(4,5-dimethylthiazol-2-yl)-5-(3-carboxymethoxyphenyl)-2-(4-sulfophenyl)-2H-tetrazolium (MTS), indicative of the mitochondrial function of living cells and cell viability, using the CellTiter96 AQueous One Solution Kit (Promega) and the Glo-Max Multi Detection System (Promega).

### *Reporter Gene Assay*

pG13-luc, containing 13 copies of a p53 DNA-binding consensus sequence linked to a luciferase reporter gene, was kindly provided by Dr. Bert Vogelstein [29]. HEK293 cells were plated at a density of  $1 \times 10^5$  cells in 24-well plates containing 500  $\mu$ L of culture medium. After incubation for 24 hrs at 37°C, cells were transfected with 100 ng pG13-luc with 10 ng Renilla pGL4.75 (hRluc-CMV) vector (Promega) as an internal control, using Lipofectamine 2000 (Life Technologies), and further incubated for 24 hrs. Next, cells were  $\gamma$ -irradiated at 20 Gy and the culture medium was changed to AMSC-CM immediately after the  $\gamma$ -irradiation. After 24 hrs, a reporter gene assay was performed using the Dual Luciferase reporter assay system (Promega) and the luminescence intensity was measured using an AB-2000 Luminescencer-PSN (Atto, Tokyo, Japan), according to the manufacturer's protocol. The transcription activity was normalized according to Renilla luciferase activity. Experiments were performed in triplicates.

### *Statistical Analysis*

Data were expressed as mean  $\pm$  SEM. Parameters among the groups were compared by



one-way ANOVA, followed by the Tukey test. Differences were considered statistically significant at a probability ( $p$ ) level  $<0.05$ .

## RESULTS

### *Characterization of Human AMSCs*

To evaluate the multipotency of human AMSCs, we induced differentiation of cultured AMSCs into osteocytes and adipocytes. AMSCs differentiated into osteocytes and adipocytes, as demonstrated by calcein and BODIPY staining, respectively (Fig. 2A). Flow cytometry of cultured AMSCs demonstrated that these cells expressed CD44, CD73, CD90, and CD105 but not CD11b, CD19, CD34, CD45, or HLA-DR, which is characteristic of MSCs (Fig. 2B) [30].

### *Effect of AMSC Transplantation on Histological Parameters in Rats with Radiation Proctitis*

Histologically, we investigated the effect of human AMSCs on the radiation proctitis model. H&E staining demonstrated that the ductal structures were destroyed and large numbers of inflammatory cells were infiltrating in the Radiation group; however, these changes were attenuated by AMSC transplantation on day 8 (Fig. 3A). In particular, histological scoring demonstrated that inflammation and mucus cell loss were significantly attenuated by AMSC transplantation (Fig. 3B). To confirm these observations, PAS staining and immunohistochemical examination were performed.

PAS staining showed that the number of goblet cells was markedly decreased by  $\gamma$ -irradiation; however, AMSC transplantation significantly attenuated the number of goblet cells (Fig. 3C). In addition, infiltration of CD68-positive monocytes/macrophages significantly increased by irradiation and was significantly attenuated by AMSC transplantation (Fig. 3D). Furthermore, infiltration of MPO-positive neutrophils significantly increased by irradiation and was significantly attenuated by AMSC transplantation (Fig. 3E).

#### *Effects of AMSC Transplantation on Gene Expression in Rats with Radiation Proctitis*

We next examined the changes in gene expression of several inflammatory cytokines in the rectum by qRT-PCR. The expression levels of CXCL1, CCL2, TNF- $\alpha$ , and IL-6 were markedly increased by  $\gamma$ -irradiation and they all tended to be decreased by AMSC transplantation, although not statistically significant (Fig. 4).

#### *Tissue Distribution of Transplanted AMSCs*

In order to confirm the existence of transplanted AMSCs, we stained the tissues with anti-human CD105 antibody. However, there were no human CD105-positive cells in the rectum, although a substantial number of AMSCs were observed in the lung (Fig. 5).

*Effect of AMSC-CM on Cell Injury of Cultured Rat Intestinal Epithelial Cells*

To determine whether radiation-induced cell injury is modulated by AMSCs, IEC-6 cells were  $\gamma$ -irradiated and then cultured with AMSC-CM. Cell proliferation, as assessed by the MTS assay, was significantly decreased by  $\gamma$ -irradiation (8 Gy); however, it was significantly affected by AMSC-CM (Fig. 6A). Marked cell death was observed by  $\gamma$ -irradiation, as demonstrated by trypan blue staining, and it was significantly attenuated by AMSC-CM (Fig. 6A). At a  $\gamma$ -irradiation of 4 Gy, cell proliferation was not inhibited by  $\gamma$ -irradiation but it significantly increased by AMSC-CM (Fig. 6B). The level of apoptosis, as determined by caspase-3/7 activity, was significantly increased by  $\gamma$ -irradiation and significantly attenuated by AMSC-CM (Fig. 6C).

*Effect of AMSC-CM on p53 Transcription Activity and Expression of p53-Target Genes*

To determine whether p53 transcription activity induced by  $\gamma$ -irradiation could be modulated by AMSC-CM, reporter gene analysis and qRT-PCR for p53-target genes were performed. Transcription activity of p53 was significantly upregulated by  $\gamma$ -irradiation; however, it was significantly decreased by AMSC-CM (Fig. 7A). qRT-PCR demonstrated that p21 and Bax expression was significantly increased by

$\gamma$ -irradiation, whereas AMSC-CM significantly decreased the expression of p21 but not Bax (Fig. 7B).

## DISCUSSION

In this study, we investigated the therapeutic potential of human AMSC transplantation in rats with radiation proctitis. We found that (1) AMSC transplantation ameliorated radiation proctitis, (2) AMSC suppressed the radiation injury of intestinal epithelial cells *in vitro*, and (3) AMSC-CM suppressed upregulation of the transcription activity of p53 as well as p21 and caspase-3/7 induced by  $\gamma$ -irradiation.

In the present study, AMSCs expressed CD44, CD73, CD90, and CD105, but not CD11b, CD19, CD34, CD45, or HLA-DR, which is characteristic of MSCs. These expression patterns were consistent with MSCs obtained from bone marrow or adipose tissue [31]. It has been demonstrated that MSCs derived from other tissues, such as bone marrow and adipose tissue, ameliorate radiation enteritis in small and large animals [32-35]. Linard *et al.* performed  $\gamma$ -irradiation (21–29 Gy) to the rectum of pigs and found that intravenous injections of autologous bone marrow-derived MSCs ( $2 \times 10^6$  cells, once a week for 3 weeks) reduced the severity of radiation-induced inflammation, resulting in a reduction of anorectal fibrosis [32]. They also demonstrated that repeated MSC injections regulate factors implicated in angiogenesis and that there was an important interplay between angiogenesis, vascular remodeling, and fibrosis. Sémont *et al.* performed  $\gamma$ -irradiation (27 Gy) to the rectum of rats and found that

repeated injections of MSCs ( $5 \times 10^6$  cells) obtained from rat bone marrow reduced the severity of radiation-induced proctitis [33]. The authors suggested that this therapeutic benefit was cell dose-dependent; the injection of lower numbers of MSCs ( $0.1 \times 10^6$  and  $1.0 \times 10^6$  cells) displayed no significant benefit on the radiation-induced epithelial injury score. They also suggested that the therapeutic benefit of MSC injections was induced by stimulating endogenous host progenitor cells to improve the regenerative process. On the other hand, Chang *et al.* performed  $\gamma$ -irradiation (15 Gy) to the whole body or abdomen of rats [34]. Rats treated with PBS or fibroblasts died within a short period after abdominal irradiation; however, most rats were rescued by intraperitoneal injection of MSCs ( $5 \times 10^6$  cells) obtained from human adipose tissue.

In the present study, we performed repeated  $\gamma$ -irradiation ( $5 \text{ Gy} \times 5 \text{ days}$ ) to the rectum of rats, which is more relevant to clinical situations, and showed that injection of only  $1 \times 10^6$  human AMSCs significantly reduced the severity of inflammation. We applied a xenotransplantation model because many reports confirmed that MSCs function across species barriers [36]. We speculate that most of the *in vivo* effects were achieved by paracrine effect, because we detected a substantial number of AMSCs in the lung, but not the rectum, after transplantation. Although the difference in characteristics among MSCs from different tissue is not thoroughly understood, one

explanation is that AMSCs produce large amounts of prostaglandin E2 (PGE<sub>2</sub>), thereby exerting robust anti-inflammatory effects [26]. In addition, we have very recently demonstrated that AMSCs can inhibit macrophage activity [27, 37]. The association between acute and late reactions is important and therefore it is possible to prevent late reactions by treating early reactions [38]. Although it is difficult to develop a chronic radiation proctitis model, our results suggest that early transplantation of AMSCs would prevent late reactions by preventing early cell injury and subsequent inflammation. Our *in vitro* experiments demonstrated that AMSC-CM suppressed cell injury induced by  $\gamma$ -irradiation in rat epithelial cells. MSCs have been reported to produce several molecules involved in cell proliferation and inhibition of cell death [33, 39, 40]. Sémont *et al.* performed *in vitro* experiments using irradiated, non-transformed rat crypt epithelial cells (IEC-18), and demonstrated that MSC-CM increased the expression of bFGF, KGF, IL-11, and wnt4 by IEC-18 [33]. They suggested that MSCs increased the number of IEC-18 cells through non-canonical WNT pathways via paracrine mechanisms. Huang *et al.* performed *in vitro* experiments using an oxygen–glucose deprivation (OGD) model, which was used to mimic ischemic injury, and demonstrated that OGD with MSC-CM could protect astrocytes from apoptosis, increase cell metabolic activity, and reduce overexpression of glial fibrillary acidic protein (GFAP)



[39]. They suggested that paracrine factors inhibited p38 MAPK and JNK, most likely by regulating the downstream targets p53 and STAT1 to promote astrocyte survival associated with GFAP downregulation after ischemic stroke.

In the present study, AMSC-CM inhibited the activation of caspase-3/7 and p53 induced by  $\gamma$ -irradiation. It has been reported that bone marrow-derived MSCs produce PGE<sub>2</sub> and protect primary B-cell precursor acute lymphoblastic leukemia (BCP-ALL) cells from p53 accumulation and apoptosis [40]. Our group has also recently demonstrated that AMSCs produce large amounts of PGE<sub>2</sub> as compared with chorion-derived MSCs, and AMSC-CM is rich in HGF, bFGF, IGF-1, and VEGF [26]. In addition, we have recently reported that AMSC-CM inhibit nuclear translocation of NF- $\kappa$ B, which is a key modulator of inflammatory signaling [27]. Although the underlying mechanism still remains to be elucidated, our results suggest that AMSC-CM could inhibit cell injury after  $\gamma$ -irradiation and subsequent inflammatory reaction.

Recent reports have suggested a similar efficacy of AMSCs in several other diseases [41-43]. It has been demonstrated that intravenous infusion of human AMSCs ameliorates inflammation and fibrosis in the lung induced by bleomycin in mice [43] and reduces liver fibrosis induced by carbon tetrachloride administration in mice [44].

Around 30 clinical trials are currently registered worldwide for evaluating MSC therapy for fibrosis [45]. Furthermore, a first-in-human clinical trial of FM-MSC transplantation in nine patients with steroid-refractory acute graft-versus-host disease (GVHD) demonstrated that the use of FM-MSCs appeared safe for intravenous infusion and the overall response rate in severe refractory acute GVHD was similar to the rate observed by using bone marrow-derived MSCs [42]. This is encouraging since aspirating bone marrow or obtaining adipose tissue from donors involves rather invasive procedures, whereas AMSCs are readily available when required by a patient, allowing storage in advance without consideration of cancer cell contamination.

In conclusion, human AMSC transplantation ameliorated radiation proctitis in rats, possibly through suppression of cell injury of epithelial cells and subsequent inflammatory response. Considering that FM is generally treated as medical waste and can be obtained without any invasive procedure, human AMSC transplantation may be a therapeutic strategy for the treatment of radiation proctitis. A clinical trial evaluating the efficacy of systemic MSC injections for the treatment of severe and chronic radiotherapy-induced abdomino-pelvic complications has been initiated in 2015 [46].

**ACKNOWLEDGEMENTS AND DISCLOSURES**

We thank Dr. Takahiro Yamada, who performed the Cesarean deliveries. This study was supported by a Grant-in Aid (C) from Japan Society for the Promotion of Science (JSPS, 23618001), and by the Health and Labour Sciences Research Grants (Research on Applying Health Technology). The authors indicate no potential conflicts of interest.

**REFERENCES**

- [1] Babb RR. Radiation proctitis: a review. *Am J Gastroenterol* 1996;91:1309-1311.
- [2] Shadad AK, Sullivan FJ, Martin JD, Egan LJ. Gastrointestinal radiation injury: symptoms, risk factors and mechanisms. *World J Gastroenterol* 2013;19:185-198.
- [3] Gilinsky NH, Burns DG, Barbezat GO, Levin W, Myers HS, Marks IN. The natural history of radiation-induced proctosigmoiditis: an analysis of 88 patients. *Q J Med* 1983;52:40-53.
- [4] Denham JW, O'Brien PC, Dunstan RH, Johansen J, See A, Hamilton CS, et al. Is there more than one late radiation proctitis syndrome? *Radiother Oncol* 1999;51:43-53.
- [5] Moore EM, Magrino TJ, Johnstone PA. Rectal bleeding after radiation therapy for prostate cancer: endoscopic evaluation. *Radiology* 2000;217:215-218.
- [6] Perez CA, Lee HK, Georgiou A, Lockett MA. Technical factors affecting morbidity in definitive irradiation for localized carcinoma of the prostate. *Int J Radiat Oncol Biol Phys* 1994;28:811-819.
- [7] Shadad AK, Sullivan FJ, Martin JD, Egan LJ. Gastrointestinal radiation injury: prevention and treatment. *World J Gastroenterol* 2013;19:199-208.
- [8] Leiper K, Morris AI. Treatment of radiation proctitis. *Clin Oncol (R Coll Radiol)* 2007;19:724-729.
- [9] Andreyev HJ, Wotherspoon A, Denham JW, Hauer-Jensen M. Defining pelvic-radiation disease for the survivorship era. *Lancet Oncol* 2010;11:310-312.
- [10] Benderitter M, Caviglioli F, Chapel A, Coppes RP, Guha C, Klinger M, et al. Stem cell therapies for the treatment of radiation-induced normal tissue side effects. *Antioxid Redox Signal* 2014;21:338-355.
- [11] Pittenger MF, Mackay AM, Beck SC, Jaiswal RK, Douglas R, Mosca JD, et al. Multilineage potential of adult human mesenchymal stem cells. *Science* 1999;284:143-147.
- [12] Meirelles Lda S, Fontes AM, Covas DT, Caplan AI. Mechanisms involved in the therapeutic properties of mesenchymal stem cells. *Cytokine Growth Factor Rev* 2009;20:419-427.
- [13] Uccelli A, Moretta L, Pistoia V. Mesenchymal stem cells in health and disease. *Nat Rev Immunol* 2008;8:726-736.
- [14] Duijvestein M, Vos AC, Roelofs H, Wildenberg ME, Wendrich BB, Verspaget HW, et al. Autologous bone marrow-derived mesenchymal stromal cell treatment for refractory luminal Crohn's disease: results of a phase I study. *Gut* 2010;59:1662-1669.
- [15] Liang J, Zhang H, Wang D, Feng X, Wang H, Hua B, et al. Allogeneic mesenchymal stem cell transplantation in seven patients with refractory inflammatory bowel disease. *Gut* 2012;61:468-469.
- [16] Voswinkel J, Francois S, Simon JM, Benderitter M, Gorin NC, Mohty M, et al. Use of mesenchymal stem cells (MSC) in chronic inflammatory fistulizing and fibrotic diseases: a

comprehensive review. *Clin Rev Allergy Immunol* 2013;45:180-192.

[17] In 't Anker PS, Noort WA, Scherjon SA, Kleijburg-van der Keur C, Kruisselbrink AB, van Bezooijen RL, et al. Mesenchymal stem cells in human second-trimester bone marrow, liver, lung, and spleen exhibit a similar immunophenotype but a heterogeneous multilineage differentiation potential. *Haematologica* 2003;88:845-852.

[18] Hu Y, Liao L, Wang Q, Ma L, Ma G, Jiang X, et al. Isolation and identification of mesenchymal stem cells from human fetal pancreas. *J Lab Clin Med* 2003;141:342-349.

[19] In 't Anker PS, Scherjon SA, Kleijburg-van der Keur C, de Groot-Swings GM, Claas FH, Fibbe WE, et al. Isolation of mesenchymal stem cells of fetal or maternal origin from human placenta. *Stem Cells* 2004;22:1338-1345.

[20] Alviano F, Fossati V, Marchionni C, Arpinati M, Bonsi L, Franchina M, et al. Term amniotic membrane is a high throughput source for multipotent mesenchymal stem cells with the ability to differentiate into endothelial cells in vitro. *BMC Dev Biol* 2007;7:11.

[21] Ishikane S, Ohnishi S, Yamahara K, Sada M, Harada K, Mishima K, et al. Allogeneic injection of fetal membrane-derived mesenchymal stem cells induces therapeutic angiogenesis in a rat model of hind limb ischemia. *Stem Cells* 2008;26:2625-2633.

[22] Ishikane S, Yamahara K, Sada M, Harada K, Kodama M, Ishibashi-Ueda H, et al. Allogeneic administration of fetal membrane-derived mesenchymal stem cells attenuates acute myocarditis in rats. *J Mol Cell Cardiol* 2010;49:753-761.

[23] Ohshima M, Yamahara K, Ishikane S, Harada K, Tsuda H, Otani K, et al. Systemic transplantation of allogenic fetal membrane-derived mesenchymal stem cells suppresses Th1 and Th17 T cell responses in experimental autoimmune myocarditis. *J Mol Cell Cardiol* 2012;53:420-428.

[24] Tsuda H, Yamahara K, Ishikane S, Otani K, Nakamura A, Sawai K, et al. Allogenic fetal membrane-derived mesenchymal stem cells contribute to renal repair in experimental glomerulonephritis. *Am J Physiol Renal Physiol* 2010;299:F1004-1013.

[25] Tsuda H, Yamahara K, Otani K, Okumi M, Yazawa K, Kaimori JY, et al. Transplantation of allogenic fetal membrane-derived mesenchymal stem cells protect against ischemia-reperfusion-induced acute kidney injury. *Cell transplantation* 2010;23:889-899.

[26] Yamahara K, Harada K, Ohshima M, Ishikane S, Ohnishi S, Tsuda H, et al. Comparison of angiogenic, cytoprotective, and immunosuppressive properties of human amnion- and chorion-derived mesenchymal stem cells. *PLoS One* 2014;9:e88319.

[27] Onishi R, Ohnishi S, Higashi R, Watari M, Yamahara K, Okubo N, et al. Human amnion-derived mesenchymal stem cell transplantation ameliorates dextran sulfate sodium-induced severe colitis in rats. *Cell Transplant* (in press).

[28] Guzman-Stein G, Bonsack M, Liberty J, Delaney JP. Abdominal radiation causes bacterial translocation. *J Surg Res* 1989;46:104-107.

- [29] El-Deiry WS, Tokino T, Velculescu VE, Levy DB, Parsons R, Trent JM, et al. WAF1, a potential mediator of p53 tumor suppression. *Cell* 1993;75:817-825.
- [30] Dominici M, Le Blanc K, Mueller I, Slaper-Cortenbach I, Marini F, Krause D, et al. Minimal criteria for defining multipotent mesenchymal stromal cells. The International Society for Cellular Therapy position statement. *Cytotherapy* 2006;8:315-317.
- [31] Nery AA, Nascimento IC, Glaser T, Bassaneze V, Krieger JE, Ulrich H. Human mesenchymal stem cells: from immunophenotyping by flow cytometry to clinical applications. *Cytometry A* 2013;83:48-61.
- [32] Linard C, Busson E, Holler V, Strup-Perrot C, Lacave-Lapalun JV, Lhomme B, et al. Repeated autologous bone marrow-derived mesenchymal stem cell injections improve radiation-induced proctitis in pigs. *Stem Cells Transl Med* 2013;2:916-927.
- [33] Sémont A, Demarquay C, Bessout R, Durand C, Benderitter M, Mathieu N. Mesenchymal stem cell therapy stimulates endogenous host progenitor cells to improve colonic epithelial regeneration. *PLoS One* 2013;8:e70170.
- [34] Chang P, Qu Y, Liu Y, Cui S, Zhu D, Wang H, et al. Multi-therapeutic effects of human adipose-derived mesenchymal stem cells on radiation-induced intestinal injury. *Cell Death Dis* 2013;4:e685.
- [35] Sémont A, Mouiseddine M, François A, Demarquay C, Mathieu N, Chapel A, et al. Mesenchymal stem cells improve small intestinal integrity through regulation of endogenous epithelial cell homeostasis. *Cell Death Differ* 2010;17:952-961.
- [36] Li J, Ezzelarab MB, Cooper DK. Do mesenchymal stem cells function across species barriers? Relevance for xenotransplantation. *Xenotransplantation* 2012;19:273-285.
- [37] Kubo K, Ohnishi S, Hosono H, Fukai M, Kameya A, Higashi R, et al. Human amnion-derived mesenchymal stem cell transplantation ameliorates liver fibrosis in rats. *Transplantation Direct* 2015;(in press).
- [38] O'Brien PC. Radiation injury of the rectum. *Radiother Oncol* 2001;60:1-14.
- [39] Huang W, Lv B, Zeng H, Shi D, Liu Y, Chen F, et al. Paracrine Factors Secreted by MSCs Promote Astrocyte Survival Associated with GFAP Downregulation After Ischemic Stroke Via p38 MAPK and JNK. *J Cell Physiol* (in press).
- [40] Naderi EH, Skah S, Ugland H, Myklebost O, Sandnes DL, Torgersen ML, et al. Bone marrow stroma-derived PGE2 protects BCP-ALL cells from DNA damage-induced p53 accumulation and cell death. *Mol Cancer* 2015;14:14.
- [41] Insausti CL, Blanquer M, Garcia-Hernandez AM, Castellanos G, Moraleda JM. Amniotic membrane-derived stem cells: immunomodulatory properties and potential clinical application. *Stem Cells Cloning* 2014;7:53-63.
- [42] Ringdén O, Erkers T, Nava S, Uzunel M, Iwarsson E, Conrad R, et al. Fetal membrane cells

for treatment of steroid-refractory acute graft-versus-host disease. *Stem Cells* 2013;31:592-601.

[43] Moodley Y, Vaghjiani V, Chan J, Baltic S, Ryan M, Tchongue J, et al. Anti-inflammatory effects of adult stem cells in sustained lung injury: a comparative study. *PLoS One* 2013;8:e69299.

[44] Zhang D, Jiang M, Miao D. Transplanted human amniotic membrane-derived mesenchymal stem cells ameliorate carbon tetrachloride-induced liver cirrhosis in mouse. *PLoS One* 2011;6:e16789.

[45] Usunier B, Benderitter M, Tamarat R, Chapel A. Management of fibrosis: the mesenchymal stromal cells breakthrough. *Stem Cells Int* 2014;2014:340257.

[46] Chapel A, Francois S, Douay L, Benderitter M, Voswinkel J. New insights for pelvic radiation disease treatment: Multipotent stromal cell is a promise mainstay treatment for the restoration of abdominopelvic severe chronic damages induced by radiotherapy. *World J Stem Cells* 2013;5:106-111.

**FIGURE LEGENDS**

**Figure 1.** Experimental protocol for the radiation proctitis model.

(A) Rats were placed in the supine position under a 6-mm thick lead shield with a 3 × 4 cm opening around the anus.

(B) Rats were  $\gamma$ -irradiated using 5 Gy/day for 5 days (day 1 through day 5) and human amnion-derived mesenchymal stem cells (AMSCs,  $1 \times 10^6$  cells) were injected intravenously on day 5. All rats were sacrificed on day 8.

**Figure 2.** Characterization of cultured human amnion-derived mesenchymal stem cells (AMSCs).

(A) Multipotency of human AMSCs. Differentiation into osteocytes was confirmed by calcein staining (upper panels). Differentiation into adipocytes was confirmed by the existence of lipid vesicles stained by BODIPY (lower panels). Scale bars, 200  $\mu$ m.

(B) Flow cytometry of human AMSCs. The negative cocktail contained antibodies against CD11b, CD19, CD34, CD45, and HLA-DR. Closed areas indicate staining with a specific antibody, whereas open areas represent staining with isotype control antibodies. Values were expressed as means  $\pm$  SEM ( $N = 3$ ).



**Figure 3.** Effect of human amnion-derived mesenchymal stem cell (AMSC) transplantation on histological parameters in rats with radiation proctitis.

(A) Hematoxylin and eosin (H&E) staining.

(B) Histological scoring.

(C) Periodic acid-Schiff (PAS) staining.

(D) CD68 staining.

(E) Myeloperoxidase (MPO) staining.

Values were expressed as means  $\pm$  SEM ( $N = 6-11$  animals/group). \* $p < 0.05$ , \*\* $p < 0.01$  vs. the Radiation group; # $p < 0.05$ , ## $p < 0.01$  vs. the Control group. Scale bars, 100  $\mu\text{m}$ .

**Figure 4.** Gene expression analysis of human amnion-derived mesenchymal stem cell (AMSC) transplantation in rats with radiation proctitis.

Quantitative reverse transcription-polymerase chain reaction (qRT-PCR) with (A) CXCL1, (B) CCL2, (C) TNF- $\alpha$ , and (D) IL-6.

Values were expressed as means  $\pm$  SEM of 6–11 animals/group. ## $p < 0.01$  vs. the Control group.

**Figure 5.** Tissue distribution of transplanted human amnion-derived mesenchymal stem cells (AMSCs).

Immunohistochemical staining with anti-human CD105 antibody in the lung (A, arrows) and rectum (B). Scale bars, 50  $\mu\text{m}$ .

**Figure 6.** Inhibition of cell injury induced by  $\gamma$ -irradiation in rat intestinal epithelial cells (IEC-6) by human amnion-derived mesenchymal stem cell-conditioned medium (AMSC-CM).

(A) MTS assay and trypan blue staining after  $\gamma$ -irradiation (8 Gy).

(B) MTS assay after  $\gamma$ -irradiation (4 Gy).

(C) Caspase-3/7 activity after  $\gamma$ -irradiation (4 Gy).

Values were expressed as means  $\pm$  SEM ( $N = 3$ ). \* $p < 0.05$ , \*\* $p < 0.01$  vs. the Radiation group;  $\#\#p < 0.01$  vs. the Control group. Scale bars, 200  $\mu\text{m}$ .

**Figure 7.** Inhibition of p53 activity induced by  $\gamma$ -irradiation by human amnion-derived mesenchymal stem cell-conditioned medium (AMSC-CM).

(A) Reporter gene assay investigating p53 transcription activity after  $\gamma$ -irradiation (4 Gy).

(B) Expression of p21 and Bax after  $\gamma$ -irradiation (4 Gy).

Values were expressed as means  $\pm$  SEM ( $N = 3$ ). \* $p < 0.05$ , \*\* $p < 0.01$  vs. the Radiation group; ### $p < 0.01$  vs. the Control group.

**Table 1.** qRT-PCR primer sequences

| Gene           | Primer sequence              |
|----------------|------------------------------|
| CCL2           | F: ATGCAGTTAATGCCCCACTC      |
|                | R: TTCCTTATTGGGGTCAGCAC      |
| CXCL1          | F: AGAACATCCAGAGTTTGAAGGTGAT |
|                | R: GTGGCTATGACTTCGGTTTGG     |
| IL-6           | F: CCCTTCAGGAACAGCTATGAA     |
|                | R: ACAACATCAGTCCCAAGAAGG     |
| TNF- $\alpha$  | F: AGAACTCCAGCGGTGTCT        |
|                | R: GAGCCCATTTGGGAACTTCT      |
| p21            | F: CACGGCTCAGTGGACCAGAA      |
|                | R: ACTGGAGCTGCCTGAGGTAGGA    |
| Bax            | F: TTGCTGATGGCAACTTCAACTG    |
|                | R: CTTTAGTGCACAGGGCCTTGAG    |
| $\beta$ -actin | F: CCAACCGTGAAAAGATGACC      |
|                | R: ACCAGAGGCATACAGGGACA      |

---

F, forward primer; R, reverse primer

Figure 1

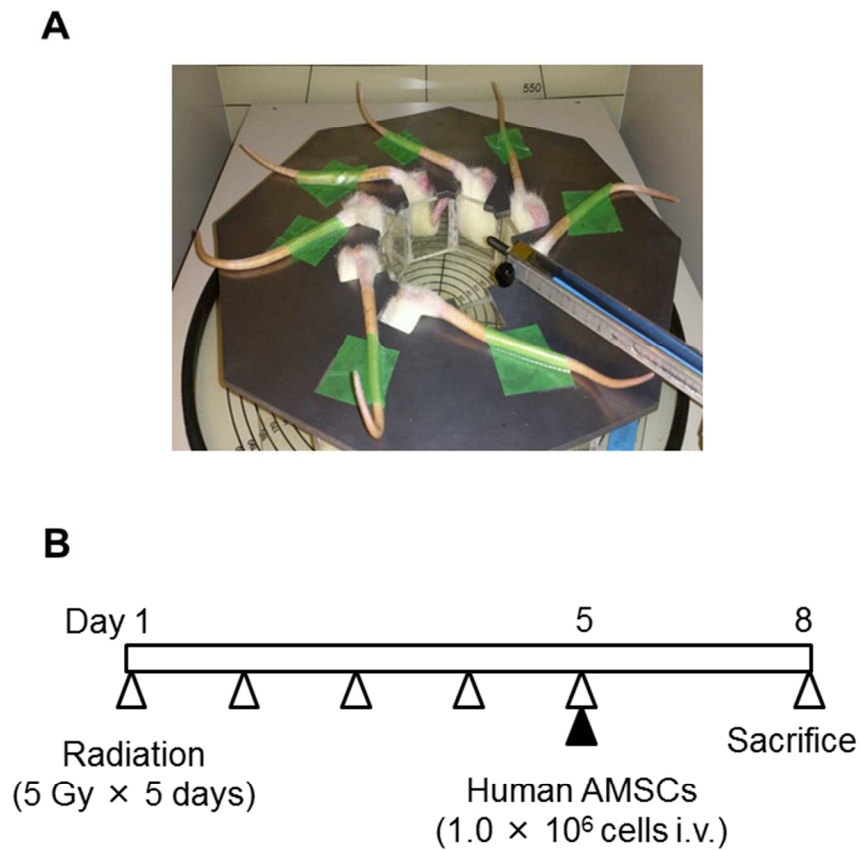


Figure 1. Experimental protocol for the radiation proctitis model.

(A) Rats were placed in the supine position under a 6-mm thick lead shield with a 3 × 4 cm opening around the anus.

(B) Rats were  $\gamma$ -irradiated using 5 Gy/day for 5 days (day 1 through day 5) and human amnion-derived mesenchymal stem cells (AMSCs,  $1 \times 10^6$  cells) were injected intravenously on day 5. All rats were sacrificed on day 8.

190x254mm (96 × 96 DPI)

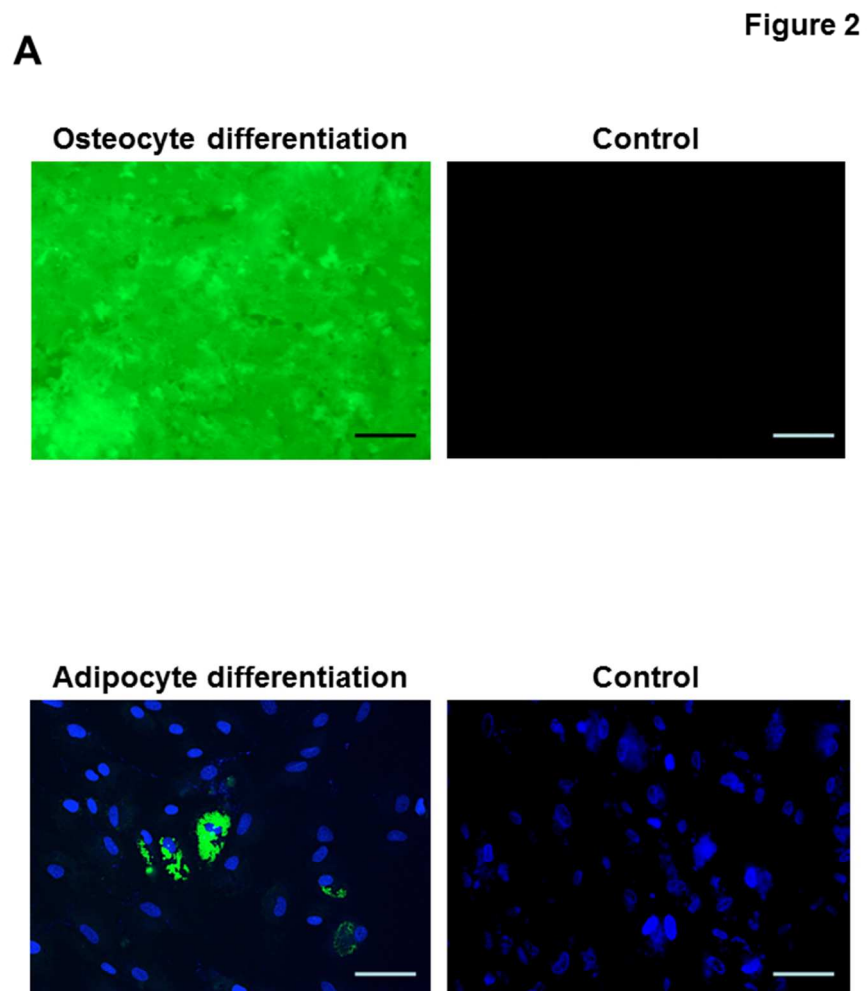


Figure 2. Characterization of cultured human amnion-derived mesenchymal stem cells (AMSCs). (A) Multipotency of human AMSCs. Differentiation into osteocytes was confirmed by calcein staining (upper panels). Differentiation into adipocytes was confirmed by the existence of lipid vesicles stained by BODIPY (lower panels). Scale bars, 200  $\mu\text{m}$ .  
190x254mm (96 x 96 DPI)

Figure 2

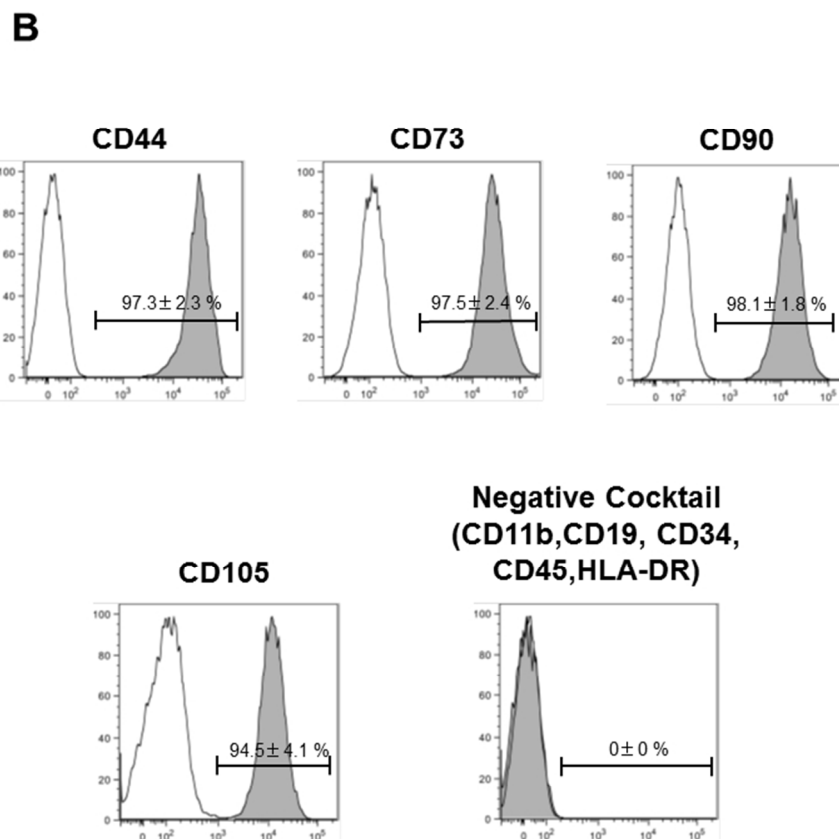


Figure 2. Characterization of cultured human amnion-derived mesenchymal stem cells (AMSCs). (B) Flow cytometry of human AMSCs. The negative cocktail contained antibodies against CD11b, CD19, CD34, CD45, and HLA-DR. Closed areas indicate staining with a specific antibody, whereas open areas represent staining with isotype control antibodies. Values were expressed as means  $\pm$  SEM (N = 3). 190x254mm (96 x 96 DPI)

Figure 3

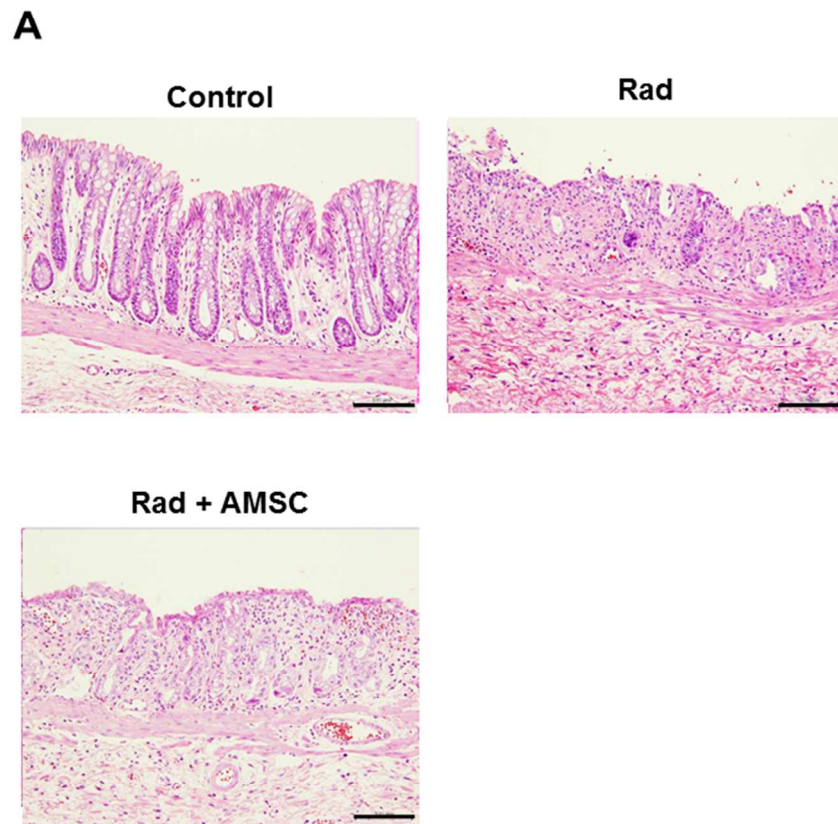


Figure 3. Effect of human amnion-derived mesenchymal stem cell (AMSC) transplantation on histological parameters in rats with radiation proctitis.

(A) Hematoxylin and eosin (H&E) staining.

Scale bars, 100  $\mu$ m.

190x254mm (96 x 96 DPI)



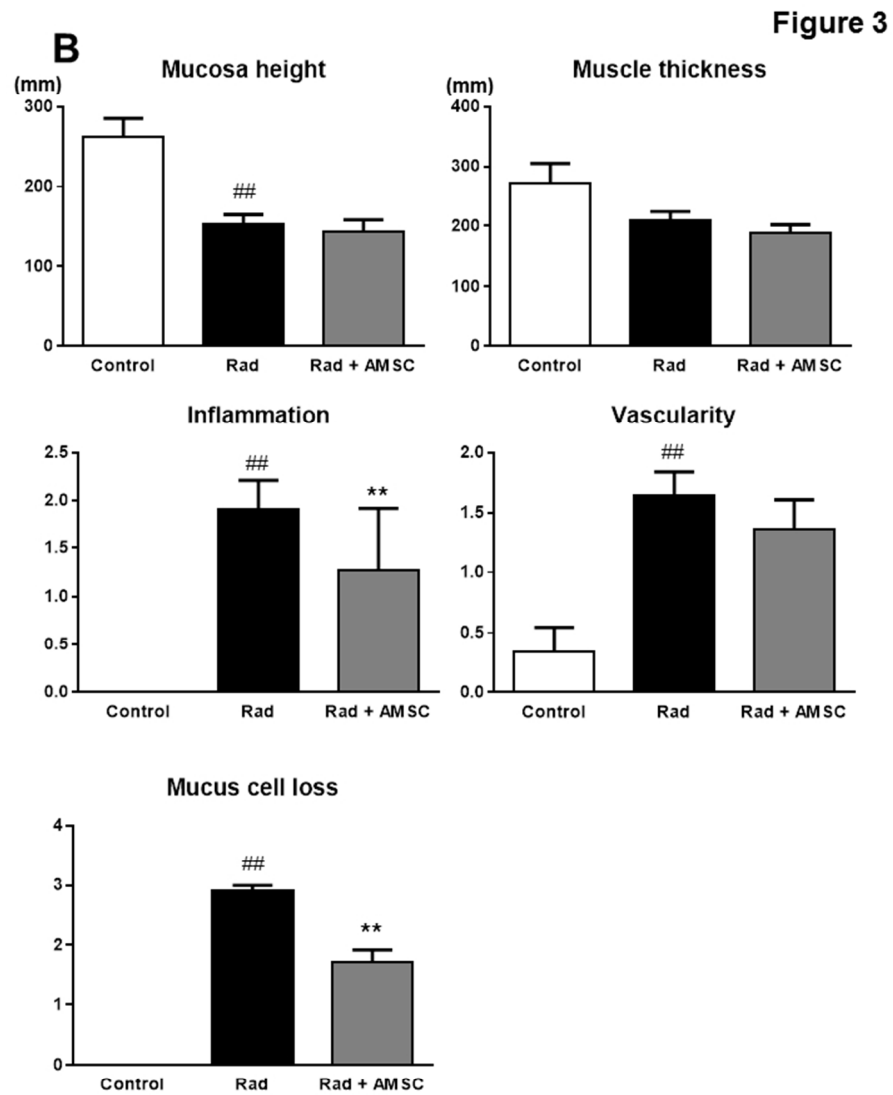


Figure 3. Effect of human amnion-derived mesenchymal stem cell (AMSC) transplantation on histological parameters in rats with radiation proctitis.

(B) Histological scoring.

Values were expressed as means  $\pm$  SEM (N = 6–11 animals/group). \*\*p < 0.01 vs. the Radiation group; ##p < 0.01 vs. the Control group.

190x254mm (96 x 96 DPI)

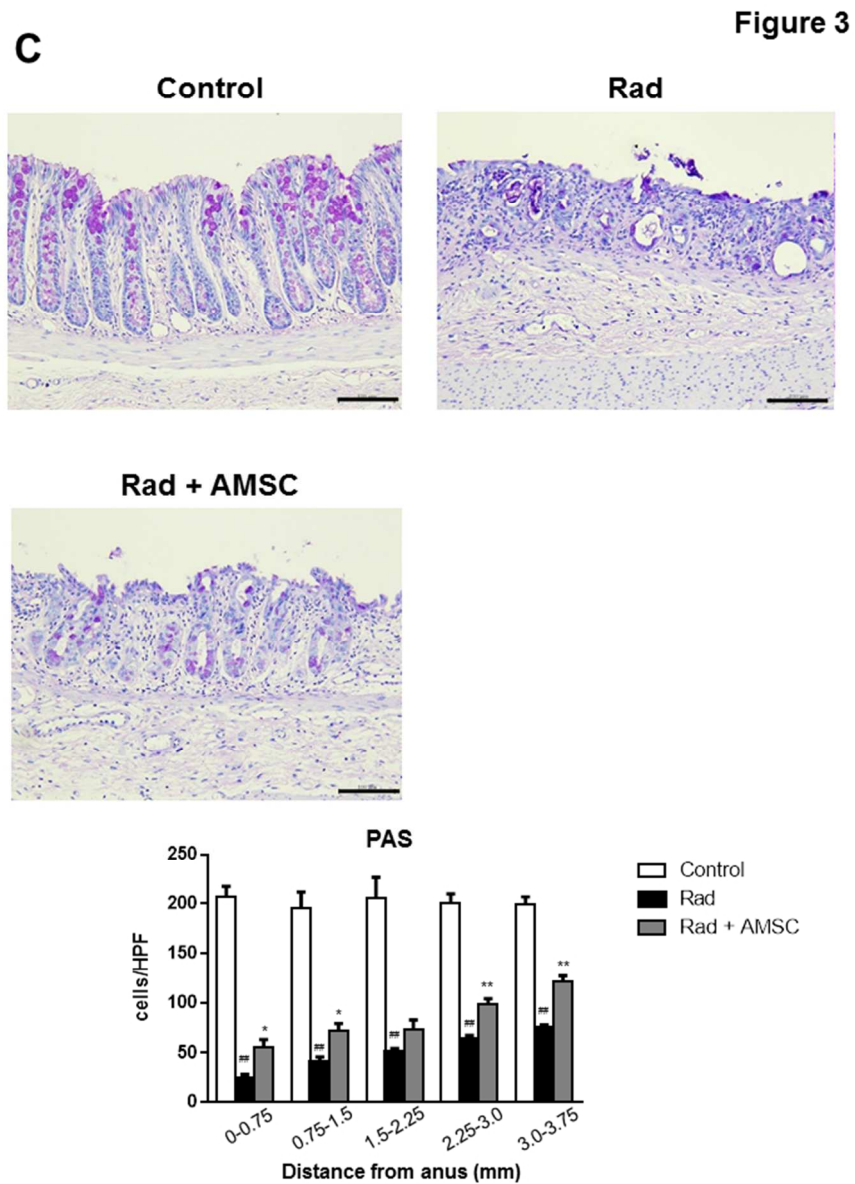


Figure 3. Effect of human amnion-derived mesenchymal stem cell (AMSC) transplantation on histological parameters in rats with radiation proctitis.

(C) Periodic acid-Schiff (PAS) staining.

Values were expressed as means  $\pm$  SEM (N = 6–11 animals/group). \*p < 0.05, \*\*p < 0.01 vs. the Radiation group; ##p < 0.01 vs. the Control group. Scale bars, 100  $\mu$ m.

190x254mm (96 x 96 DPI)

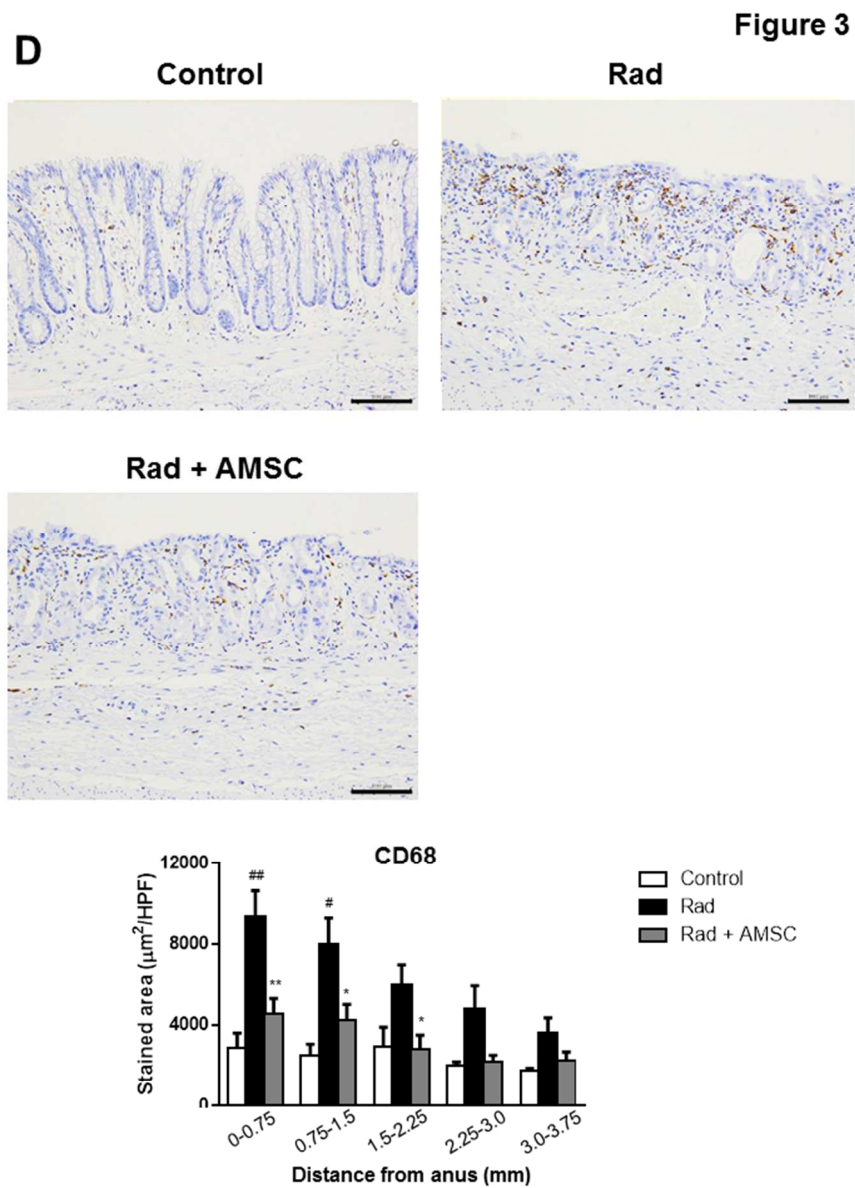


Figure 3. Effect of human amnion-derived mesenchymal stem cell (AMSC) transplantation on histological parameters in rats with radiation proctitis

(D) CD68 staining.

Values were expressed as means  $\pm$  SEM (N = 6–11 animals/group). \*p < 0.05, \*\*p < 0.01 vs. the Radiation group; #p < 0.05, ##p < 0.01 vs. the Control group. Scale bars, 100  $\mu\text{m}$ .

190x254mm (96 x 96 DPI)

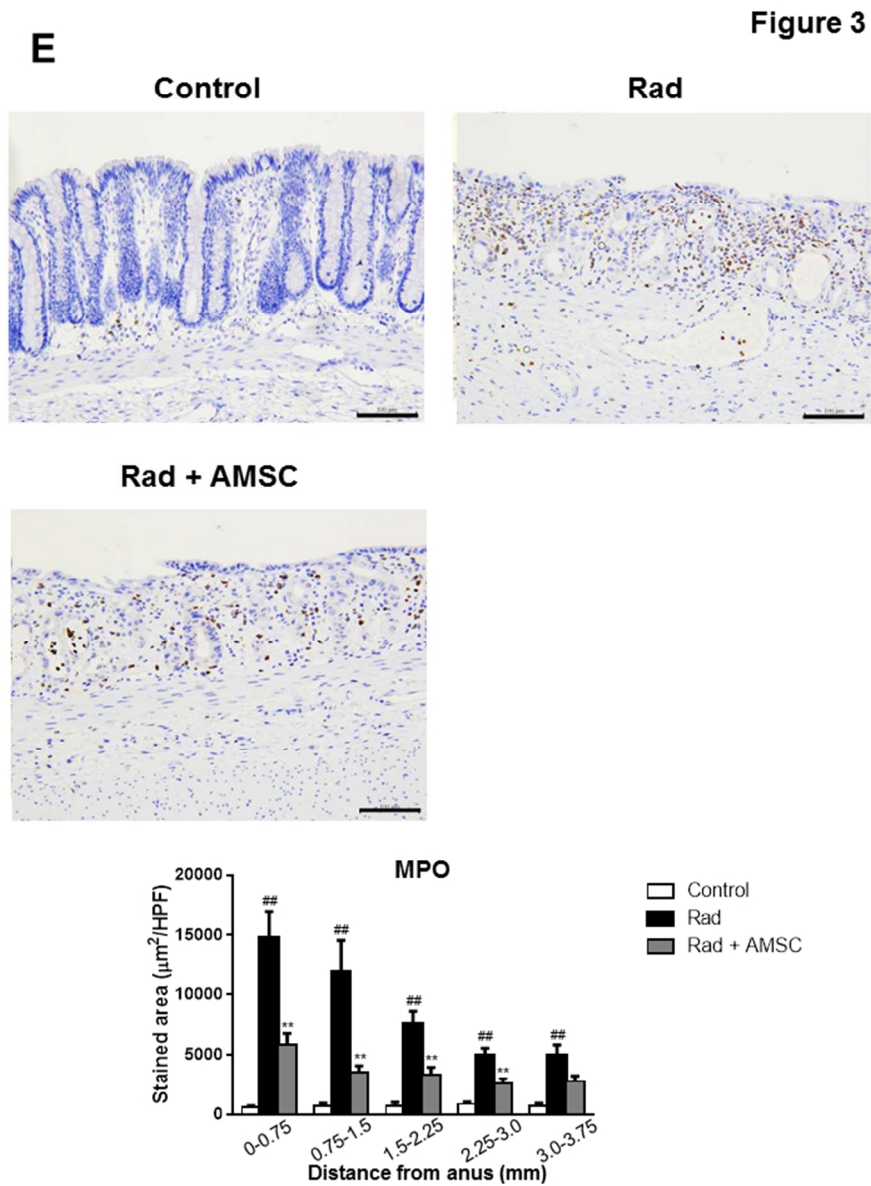


Figure 3. Effect of human amnion-derived mesenchymal stem cell (AMSC) transplantation on histological parameters in rats with radiation proctitis.

(E) Myeloperoxidase (MPO) staining.

Values were expressed as means  $\pm$  SEM (N = 6–11 animals/group). \*\*p < 0.01 vs. the Radiation group; ##p < 0.01 vs. the Control group. Scale bars, 100  $\mu$ m. 190x254mm (96 x 96 DPI)

Figure 4

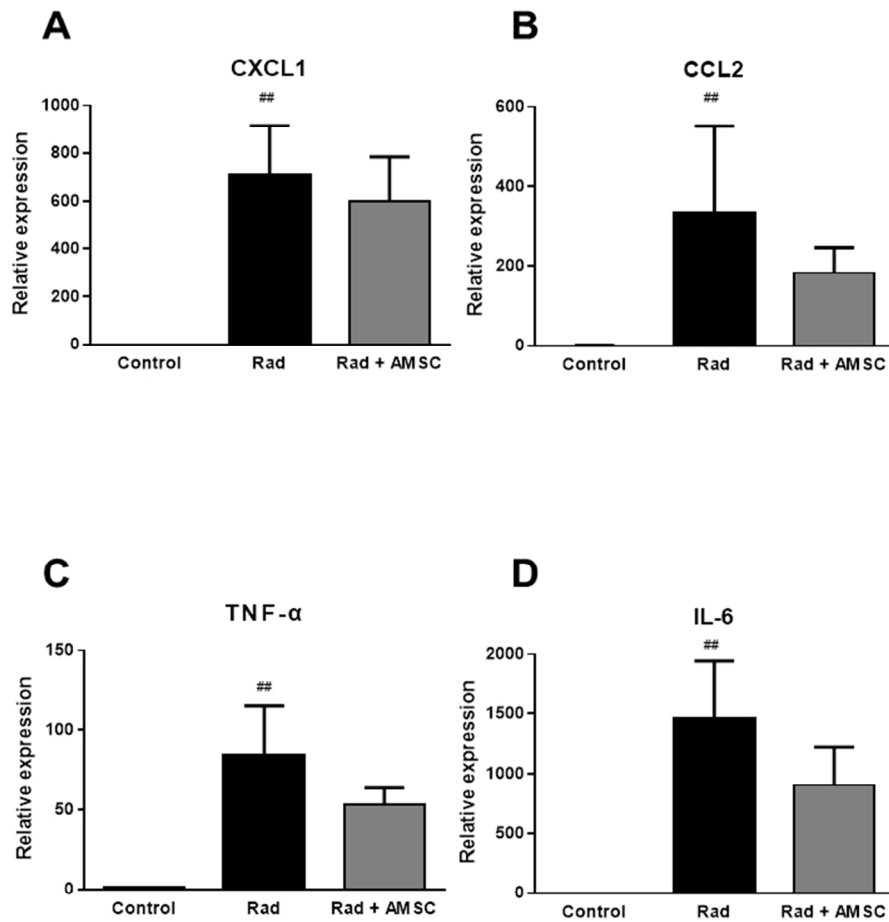


Figure 4. Gene expression analysis of human amnion-derived mesenchymal stem cell (AMSC) transplantation in rats with radiation proctitis. Quantitative reverse transcription-polymerase chain reaction (qRT-PCR) with (A) CXCL1, (B) CCL2, (C) TNF- $\alpha$ , and (D) IL-6.

Values were expressed as means  $\pm$  SEM of 6–11 animals/group. ## $p < 0.01$  vs. the Control group. 190x254mm (96 x 96 DPI)

Figure 5

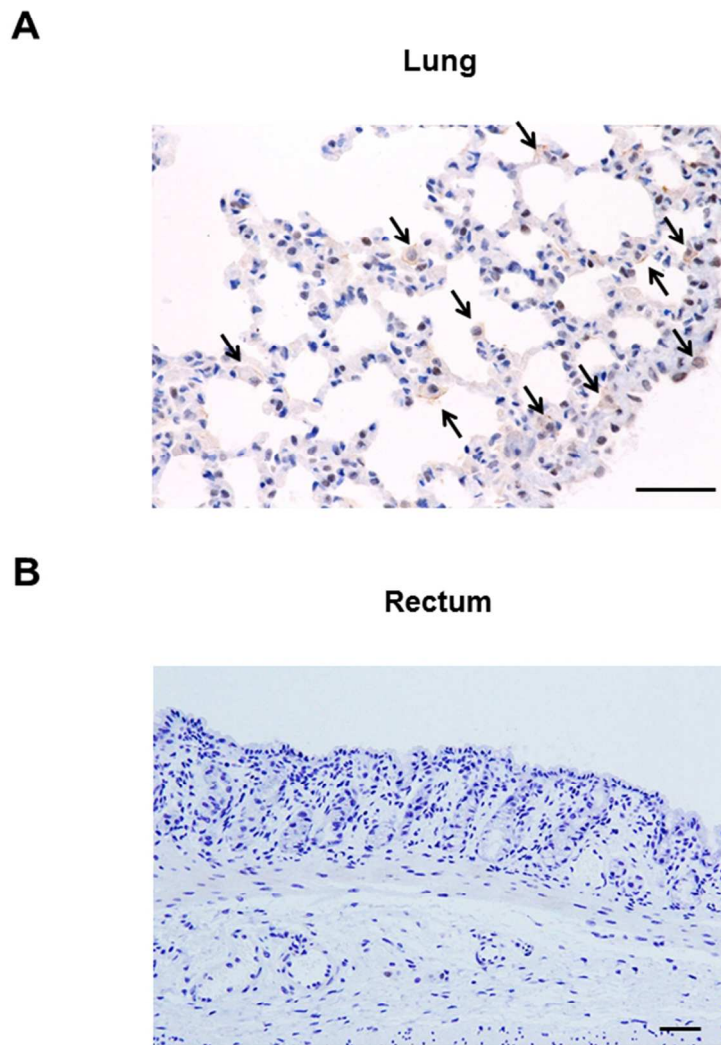


Figure 5. Tissue distribution of transplanted human amnion-derived mesenchymal stem cells (AMSCs). Immunohistochemical staining with anti-human CD105 antibody in the lung (A, arrows) and rectum (B). Scale bars, 50  $\mu$ m. 190x254mm (96 x 96 DPI)

Figure 6

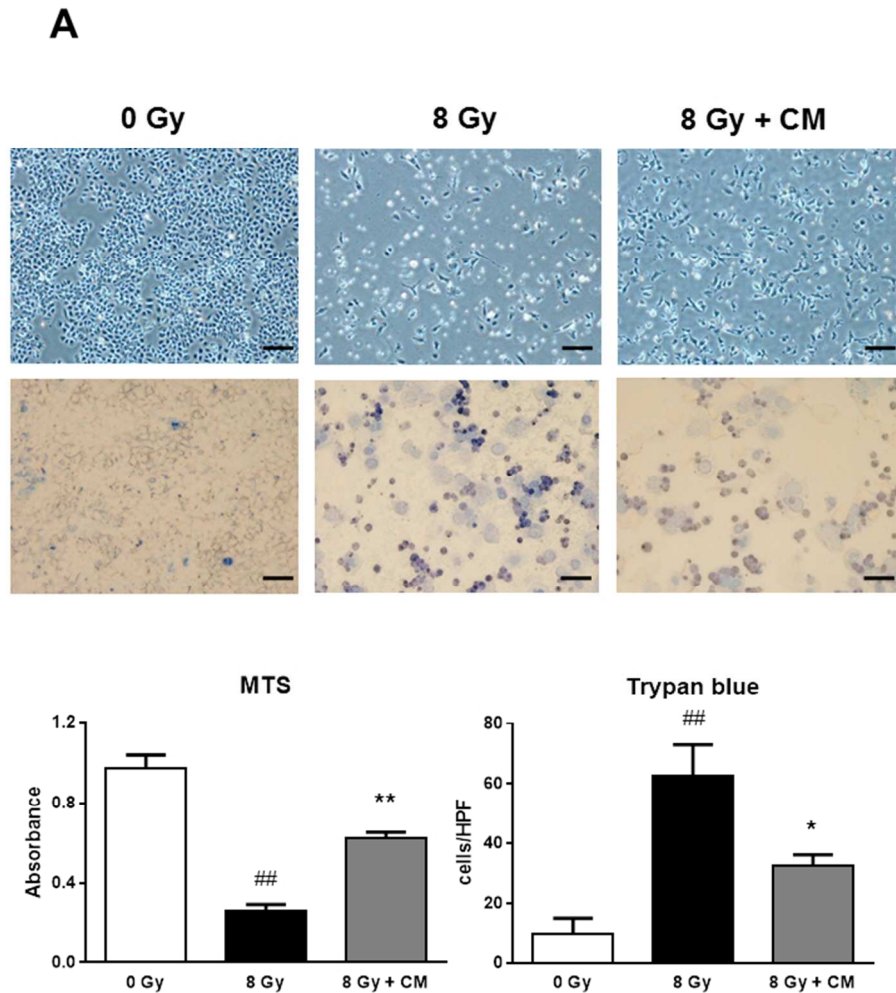


Figure 6. Inhibition of cell injury induced by  $\gamma$ -irradiation in rat intestinal epithelial cells (IEC-6) by human amnion-derived mesenchymal stem cell-conditioned medium (AMSC-CM).  
 (A) MTS assay and trypan blue staining after  $\gamma$ -irradiation (8 Gy).  
 Values were expressed as means  $\pm$  SEM (N = 3). \* $p$  < 0.05, \*\* $p$  < 0.01 vs. the Radiation group; ## $p$  < 0.01 vs. the Control group. Scale bars, 200  $\mu$ m.  
 190x254mm (96 x 96 DPI)

Figure 6

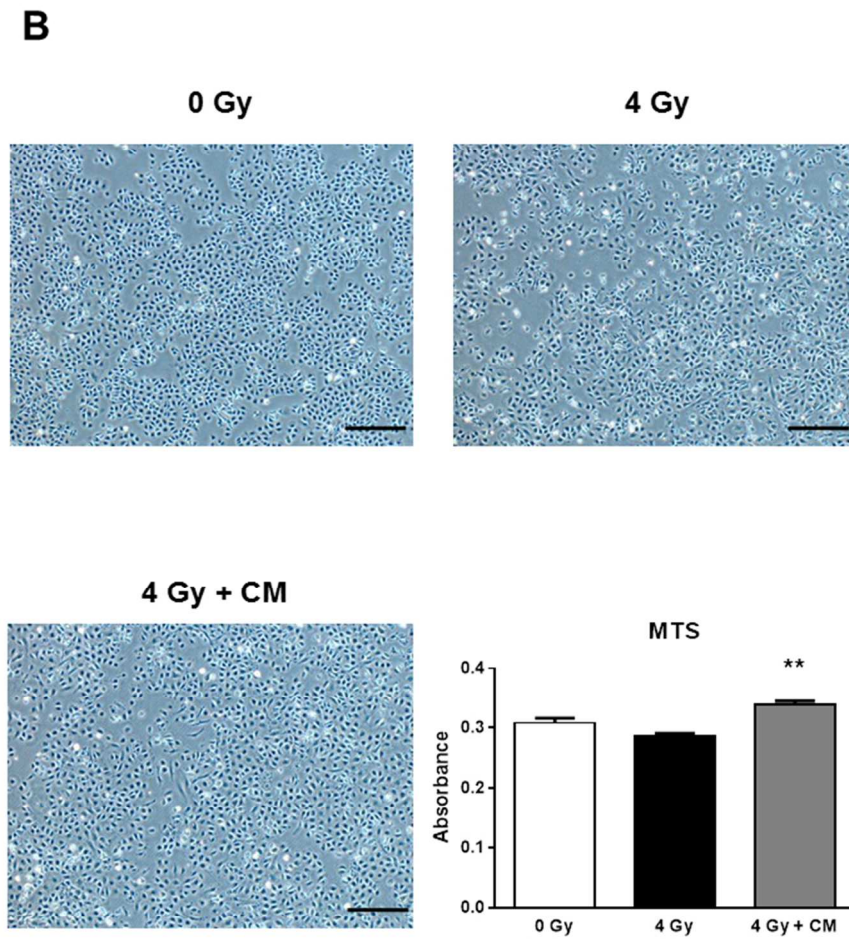


Figure 6. Inhibition of cell injury induced by  $\gamma$ -irradiation in rat intestinal epithelial cells (IEC-6) by human amnion-derived mesenchymal stem cell-conditioned medium (AMSC-CM).

(B) MTS assay after  $\gamma$ -irradiation (4 Gy).

Values were expressed as means  $\pm$  SEM (N = 3). \*\*p < 0.01 vs. the Radiation group. Scale bars, 200  $\mu$ m. 190x254mm (96 x 96 DPI)



C

Figure 6

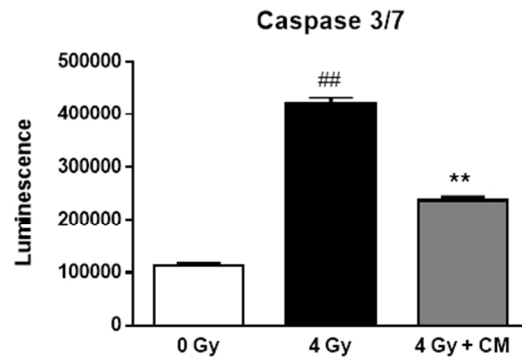


Figure 6. Inhibition of cell injury induced by  $\gamma$ -irradiation in rat intestinal epithelial cells (IEC-6) by human amnion-derived mesenchymal stem cell-conditioned medium (AMSC-CM).

(C) Caspase-3/7 activity after  $\gamma$ -irradiation (4 Gy).

Values were expressed as means  $\pm$  SEM (N = 3). \*\*p < 0.01 vs. the Radiation group; ##p < 0.01 vs. the Control group.

190x254mm (96 x 96 DPI)

Figure 7

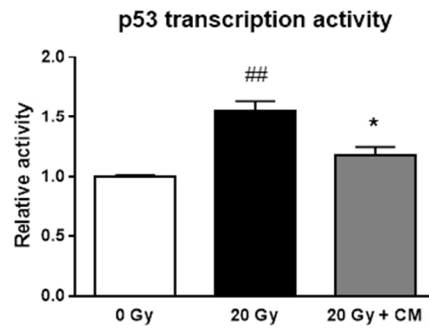
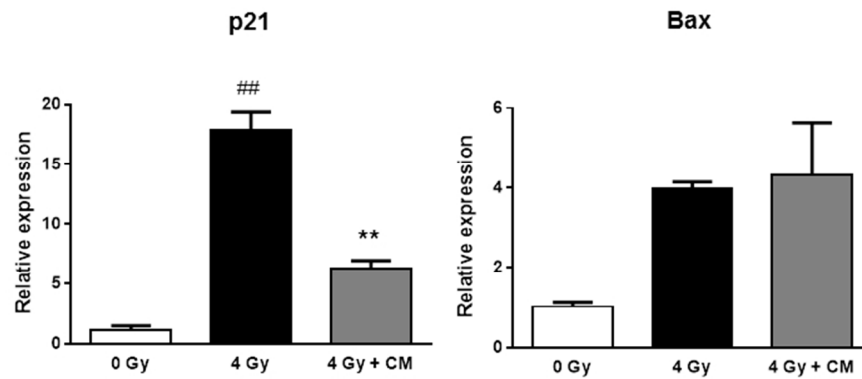
**A****B**

Figure 7. Inhibition of p53 activity induced by  $\gamma$ -irradiation by human amnion-derived mesenchymal stem cell-conditioned medium (AMSC-CM).

(A) Reporter gene assay investigating p53 transcription activity after  $\gamma$ -irradiation (4 Gy).

(B) Expression of p21 and Bax after  $\gamma$ -irradiation (4 Gy).

Values were expressed as means  $\pm$  SEM (N = 3). \*p < 0.05, \*\*p < 0.01 vs. the Radiation group; ##p < 0.01 vs. the Control group.

190x254mm (96 x 96 DPI)